Journal of Neuroimmunology 344 (2020) 577249

Contents lists available at ScienceDirect

Journal of Neuroimmunology

journal homepage: www.elsevier.com/locate/jneuroim

Examination and characterisation of burst spinal cord stimulation on cerebrospinal fluid cellular and protein constituents in patient responders with chronic neuropathic pain - A Pilot Study

Jonathan Royds[a,*], Melissa J. Conroy[b], Margaret R. Dunne[b], Hilary Cassidy[c], David Matallanas[c], Joanne Lysaght[b], Connail McCrory[a]

[a] Department of Pain Medicine, St. James Hospital, Dublin and School of Medicine, Trinity College Dublin, Ireland
[b] Department of Surgery, Trinity Translational Medicine Institute, St. James's Hospital and Trinity College Dublin, Dublin 8, Ireland
[c] Systems Biology Ireland, School of Medicine, University College Dublin, Dublin 4, Ireland

ARTICLE INFO

Keywords:
Spinal cord stimulation
Neural interface
Neuropathic pain
Neuroimmune

ABSTRACT

Introduction: Patients with neuropathic pain have altered proteomic and neuropeptide constituents in cerebrospinal fluid (CSF) compared to controls. Tonic spinal cord stimulation (SCS) has demonstrated differential expression of neuropeptides in CSF before and after treatment suggesting potential mechanisms of action. Burst-SCS is an evidence-based paraesthesia free waveform utilised for neuropathic pain with a potentially different mechanistic action to tonic SCS. This study examines the dynamic biological changes of CSF at a cellular and proteome level after Burst-SCS.

Methods: Patients with neuropathic pain selected for SCS had CSF sampled prior to implant of SCS and following 8 weeks of continuous Burst-SCS. Baseline and 8-week pain scores with demographics were recorded. T cell frequencies were analysed by flow cytometry, proteome analysis was performed using mass spectrometry and secreted cytokines, chemokines and neurotrophins were measured by enzyme-linked immunosorbent assay (ELISA).

Results: 4 patients (2 females, 2 males) with a mean age of 51 years (+/-SEM 2.74, SD 5.48) achieved a reduction in pain of >50% following 8 weeks of Burst-SCS. Analysis of the CSF proteome indicated a significant alteration in protein expression most related to synapse assembly and immune regulators. There was significantly lower expression of the proteins: growth hormone A1 (PRL), somatostatin (SST), nucleobindin-2 (NUCB2), Calbindin (CALB1), acyl-CoA binding protein (DBI), proSAAS (PCSK1N), endothelin-3 (END3) and cholecystokinin (CCK) after Burst-SCS. The concentrations of secreted chemokines and cytokines and the frequencies of T cells were not significantly changed following Burst-SCS.

Conclusion: This study characterised the alteration in the CSF proteome in response to burst SCS in vivo. Functional analysis indicated that the alterations in the CSF proteome is predominately linked to synapse assembly and immune effectors. Individual protein analysis also suggests potential supraspinal mechanisms.

1. Introduction

Burst-DR Spinal Cord Stimulation (SCS) (Abbott, Plano, TX), first introduced by De Ridder, is a paraesthesia-free based waveform utilised in patients with chronic neuropathic pain refractory to medical therapy (De Ridder et al., 2010). Burst-SCS has demonstrated non-inferiority to tonic, paraesthesia-based-stimulation in a randomised controlled study in patients with Failed Back Surgery Syndrome (FBSS) (Deer et al., 2018). Burst-SCS may also be considered when tonic stimulation has intolerable side effects or fails to achieve efficacy (Courtney et al., 2015; Tjepkema-Cloostermans et al., 2016).

In Burst-SCS, 5 pulses are delivered per burst at a frequency of 500 Hz, with 40 bursts applied per second (Bocci et al., 2018; De Ridder and Vanneste, 2016). Pre-clinical and in vitro evidence has portrayed burst neuronal firing (BNF) in sensory transmission as relaying stimuli dependent information. BNF can also improve signal to noise ratio and

Abbreviations: BNF, Burst Neuronal Firing; CSF, Cerebrospinal Fluid; CNS, Central Nervous System; ELISA, Enzyme-linked immunosorbent assay; FBSS, Failed Back Surgery Syndrome; NRS, Numerical Rating score; SCS, Spinal Cord Stimulation; TSPO, Translocator protein

* Corresponding author at: Department of Pain Medicine, St. James's Hospital, Dublin 8, Ireland.
E-mail address: roydsj@tcd.ie (J. Royds).

https://doi.org/10.1016/j.jneuroim.2020.577249
Received 28 November 2019; Received in revised form 11 March 2020; Accepted 21 April 2020

can increase the reliability of synaptic transmission and efficacy (Krahe and Gabbiani, 2004). Behaviourally relevant stimulus features may also be involved with BNF and there is evidence to suggest Burst-SCS activates the medial spinothalamic tract and may improve the behavioural and emotional component of chronic neuropathic pain in humans (De Ridder and Vanneste, 2016; Krahe and Gabbiani, 2004; Yearwood et al., 2019). The full extent of Burst-SCS in modulating the sensory information in chronic pain however remains to be defined.

There is growing evidence that the mechanism of action of Spinal Cord Stimulation (SCS) is not dependent solely on neuronal discharge but also on alterations in the Central Nervous System (CNS) cellular function (Ahmed et al., 2018; Caylor et al., 2019; Chakravarthy et al., 2018; Kinfe et al., 2017; Kriek et al., 2018; Lind et al., 2016; McCarthy et al., 2013; Vallejo et al., 2017). The concept of micro-dosing, now utilised with Burst-SCS, where there is a prolonged period between stimulation doses may also indicate mechanisms beyond neuronal discharge (Vesper et al., 2019). The syncytium of neuronal cells in the spinal cord where SCS is applied for back and leg pain contains predominantly glial cells of a ratio ranging from 11 to 13:1 compared to neurons (Ruiz-Sauri et al., 2019). BNF has elicited differential effects in neuronal-glia communications in pre-clinical studies further enhancing a wider mechanistic profile (Cacace et al., 2017; Cui et al., 2018; Fields and Burnstock, 2006). There is also increasing evidence that chronic neuropathic pain is also not solely related to neuronal pathology but also includes pathological neuronal-glia communications (Inoue and Tsuda, 2018; Ji et al., 2018; Tsuda et al., 2017; Zhao et al., 2017).

Examination of CSF has been used in many conditions including chronic neuropathic pain to help determine pathogenesis and mechanisms of treatment (Korvela et al., 2016; Kothur et al., 2016; Lind et al., 2016; McCarthy et al., 2013; McCarthy and McCrory, 2014). We thus carried out a study to examine the effect of Burst-SCS on patients with a diagnosis of neuropathic pain. Examination and characterisation of proteomic and cellular profiles before and after Burst-SCS will help to develop our understanding of the mechanism of action of this modality of spinal cord stimulation and provide much needed information on the pathophysiology of neuropathic pain in vivo (Caylor et al., 2019; Chakravarthy et al., 2019). Neuropathic pain is recognised as the type of chronic pain which has proven most resistant to current pharmacological therapies as a result of the pathological alterations in CNS physiology (Finnerup et al., 2015). At present the exact mechanisms underpinning this resistance to treatment remain unclear (Colloca et al., 2017; Meacham et al., 2017). Although there are no high quality sham/placebo controlled trials, electrical neuromodulation has demonstrated a significant improvement in multidimensional outcomes for chronic neuropathic pain patients (Deer et al., 2018; Deer et al., 2017; Kapural et al., 2016; Mekhail et al., 2019).

2. Methods

2.1. Study design

This was an interventional prospective study performed in St James's Hospital, Dublin 8, Ireland; a tertiary referral centre for patients with chronic pain. Ethical approval was obtained from the St James's and AMNCH Research Ethics Committee, Dublin, Ireland. The study was registered online at http://www.isrctn.com/ISRCTN70120536. Patients were offered inclusion following an outpatient pain clinic assessment to determine whether the patient met the inclusion/exclusion criteria.

Inclusion criteria included (i) patients must be aged between 20 and 65 years, (ii) patients must present with neuropathic pain (iii) patients must have been approved by the Department of Pain Medicine for spinal cord stimulation, (iv) patients must have had an MRI of their spine and finally (v) patients must have achieved a reduction in Numerical Rating Pain score (NRS) of 50% after eight weeks of Burst-SCS. This is the standard method to measure if a patient is classified as a responder in the majority of studies utilising electrical neuromodulation (Deer et al., 2018; Deer et al., 2017; Kapural et al., 2016; Mekhail et al., 2019).

Exclusion criteria included (i) patient refusal, (ii) if the patient was receiving anticoagulant medication, (iii) if the patient was shown to have an ongoing infection, (iv) if the patient was pregnant or breast-feeding, (v) if the patient had previously had a stroke, (vi) if the patient has a psychiatric history, (vii) if the patient has a cognitive impairment, and finally (viii) if the patient is currently medicated with biologic medication, anti-inflammatory medication or immunosuppressive therapy.

All patients were given an information leaflet about inclusion in the study as per ethics committee. All patients provided a signed a consent form in agreement with the Hospital ethics committee's requirements for study inclusion. Additionally, signed consent forms were required for the lumbar punctures for CSF sampling. Patients were instructed not to reduce their medications until after completion of the study.

2.2. CSF sampling

The baseline CSF sampling occurred between 13:00–14:00 with the patients required to fast for 13–14 h prior to implant of the SCS device. Under strict asepsis and AAGBI guidelines (Association of Anaesthetists of Great et al., 2014), CSF was obtained between the fourth and fifth lumbar vertebra using Ultrasound or Fluoroscopy. Prior to performing the lumbar puncture (LP), 2-3 ml of Lidocaine (1%) was allowed to infiltrate the skin at the site to provide local analgesia. LP was performed with an introducer and 25 Gauge Whittacre needle (B braun®) until resistance entering the dura was felt. The CSF was collected in cryovials for subsequent ELISA and mass spectrometry. The CSF sample intended for flow cytometric analysis was stored in a Transfix/EDTA tube (CaltagMedisystems, Buckingham, UK). The acquired CSF samples were visually inspected for blood contamination. To ensure there was no blood contamination the proteomics aliquots were centrifuged for 10 min at 2000*g* at 4 °C and the supernatant was transferred to a new tube. The Transfix tube was placed in storage at 4 °C and the other tubes were immediately frozen at −20 degrees Celsius. A second consented LP sample was obtained in the same manner 8 weeks after the implantation of the SCS.

2.3. Pain measurement

Each patient completed an average 24-h numerical rating score (NRS) (Hawker et al., 2011) and a Douleur Neuropathique score (DN4) (Bouhassira et al., 2005) by the investigating physician prior to obtaining the initial CSF sample. The NRS and DN4 assessment was repeated following SCS treatment for 8 weeks. The patients were instructed to remain on their current medications until the second CSF sample was taken. Positive responders were deemed as those who reported a > 50% reduction in pain in the NRS questionnaire after 8 weeks of Burst-SCS which is frequently utilised as a responder to therapy in SCS trials (Deer et al., 2018; Kapural et al., 2016; Mekhail et al., 2019).

2.4. Intervention

Patients were implanted with leads in the epidural space with paraesthesia mapping to ensure the stimulation was covering the affected area of pain. There was no trial period of stimulation and the implantable programme generator (IPG) was placed in the buttock after intra-operative stimulation (Weinand et al., 2003). All of the patients implanted devices were programmed the day after surgery with a Burst-SCS protocol which was implemented for 8 weeks until the second pain NRS assessment was performed and the second CSF sample was obtained via LP.

2.5. Quantification of T cells in CSF

After collection, samples were stored at 4 °C for no longer than 72 h in TransFix/EDTA CSF Sample Storage Tubes (Caltag Medsystems Ltd., Buckingham, UK). Samples were brought to room temperature and washed in phosphate buffered saline (PBS) solution was added to each tube and the samples were centrifuged at 1500 rpm for 3 min. The supernatant was discarded and the Transfix tube vortexed. The pellet in the Transfix tube was re-suspended in 200 µl of PBS and stained with fluorochrome-conjugated monoclonal antibodies (mAbs) specific for human surface markers (CD45-APC, CD3-APC-Vio770, CD8-PerCP, CD69-PE, CD45RA-VioGreen, CD27-VioBright FITC) obtained from Miltenyi Biotec (Germany). incubated in the dark for 30 min at 4 °C. 2mls of PBS were added to each tube and centrifuged at 1500 rpm for 3 min, then washed in PBS. Due to the precious nature of the CSF samples and the lower number of cells within each CSF sample, flow cytometry voltage and compensation settings were optimised for this lymphocyte antibody panel using peripheral blood lymphocytes. Patient-matched unstained CSF samples were used as a control for each experiment. Data was acquired using a CyAn™ ADP Analyzer (Beckman Coulter) and Summit v4.1 and analysed using FlowJo v7.6.1 (Tree Star Inc.). An example of the gating method used is demonstrated in Fig. 1. For every sample, Forward Scatter (FSC) v Side Scatter (SSC) dot plots were used to gate on lymphocytes based on size and granularity (Fig. 1A), followed by gating on cells expressing the lymphocyte common antigen CD45 (Fig. 1B). All $CD45^+$ cells expressing CD3 were gated to identify the total T cell population (Fig. 1C). Subsequent gating within this $CD3^+CD45^+$ population facilitated the identification of $CD8^+$ T cells, $CD69^+$ T cells and the 4 different T cell memory subsets; naive, central memory, effector memory and terminally differentiated, based on CD45RA and CD27 expression (Fig. 1D).

2.6. Quantification of soluble mediators in CSF

Glial Cell Derived Neurotrophic factor (GDNF) and Fractalkine single plex ELISAs (Abcam, Cambridge, UK) were performed according to the manufacturer's guidelines. Mesoscale Diagnostics (MSD, Rockville, MD, USA) V-Plex Human Cytokine 30-Plex kit, R-Plex Human Brain Derived Neurotrophic factor (BDNF) antibody set with MSD Gold 96 SM Spot Streptavidin plate pack, and human Nerve Growth Factor (NGF) ELISAs were performed as per the manufacturer's instructions, using a final CSF dilution of 1:2. MSD plates were read using MesoScale Diagnostics Sector S600. The sensitivities to the kits are available at www.mesoscale.com and www.abcam.com. The limits of detection for the neuropeptides were in pg/ml: GM-CSF 0.842-750, IL-1α 2.85-278, IL-5 4.41-562, IL-7 0.546-563, IL-12/IL-23p40 1.32-2250, IL-15 0.774-525, IL-16 19.1-1870, IL-17A 3.19-3650, TNF-β 0.465-458, VEGF-A 7.70-562, IFN-γ 1.76-938, IL-1β 0.646-375, IL-2 0.890-938, IL-4 0.218-158, IL-6 0.633-488, IL-8 0.591-375, IL-10 0.298-233, IL-12p70 1.22-315, IL-13 4.21-353, TNF-α 0.690-248,

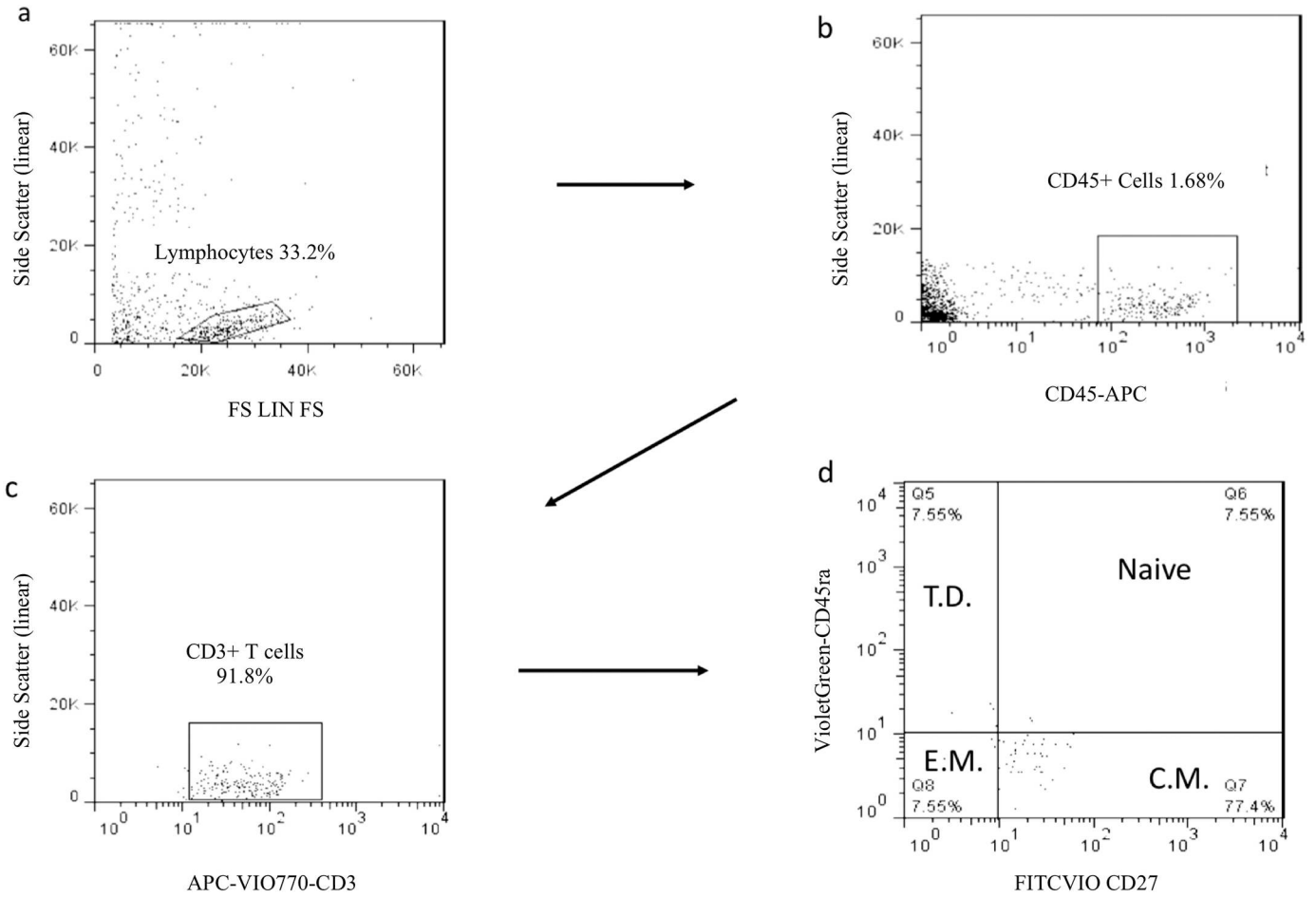

Fig. 1. Gating strategy used for T Cells. Forward Scatter (FSC) v Side Scatter (SSC) dot plots were used to gate on lymphocytes based on size and granularity (Fig. 1a), followed by gating on cells expressing the lymphocyte common antigen CD45 (Fig. 1b). All $CD45^+$ cells expressing CD3 were gated to identify the total T cell population (Fig. 1c). Subsequent gating within this $CD3^+CD45^+$ population facilitated the identification of $CD8^+$ T cells, $CD69^+$ T cells and the 4 different T cell memory subsets; naive, central memory(C.M), effector memory (E.M) and terminally differentiated (T.D) (Fig. 1d). Data was acquired using a CyAn™ ADP Analyzer (Beckman Coulter) and Summit v4.1 and analysed using FlowJo v7.6.1. (For interpretation of the references to colour in this figure legend, the reader is referred to the web version of this article.)

Table 1
Distribution of Patient Characteristics prior to implant of Spinal cord Stimulator: Age, Gender, Diagnosis, Douleur Neuropathique score (DN4), Area of Pain, Medications and quantity taken in mg. FBSS: Failed back surgery syndrome; FNSS: Failed Neck Surgery Syndrome.

Study ID	Age	Gender	Diagnosis	DN4 Score	Area of pain	Medications (per day)
101	45	Male	FNSS (cervical fusion)	4	Left neck and arm	None
102	57	Female	FBSS	9	Left back and leg	Targin 20 mg/200 mg (oxycodone/naloxone)
103	48	Male	FBSS	9	Left back and leg	None
104	54	Female	Chronic post mastectomy pain	7	T4, 5 dermatomes	Pregabalin 150 mg/ day

Table 2
Spinal cord stimulator (SCS) settings and 24 h Numerical Pain Scores (NRS) before and after Burst-SCS Stimulation for 8 weeks: Patients were deemed responders to Burst-SCS stimulation if a 50% reduction in pain occurred.

Study ID	Electrode type	Contacts	Burst rate (Hz)	Intraburst rate (Hz)	Burst spike pulse width (ms)	Target amplitude (mA)	Baseline NRS	NRS with Burst-SCS for 8 weeks
101	Octrode x 1	1-,3+,5+,6-	40	500	1	0.6	7	0
102	Octrode x 2	14-, 15+, 16-	40	500	1	0.6	8	4
103	Octrode x 2	13+, 14-	40	500	1	0.6	8	3
104	Octrode x 2	7+, 9-, 8+	40	500	1	0.55	8	3

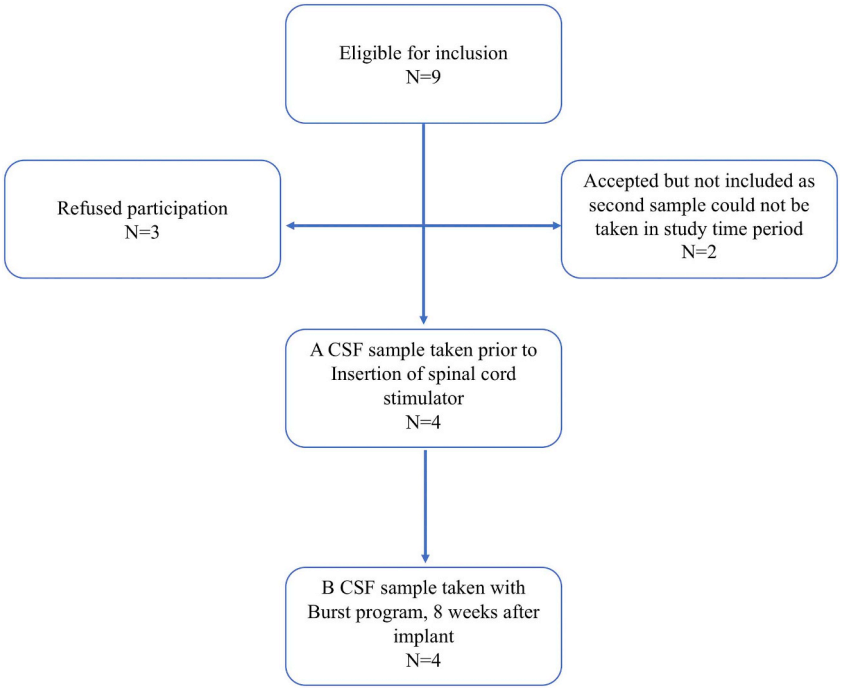

Fig. 2. Consort diagram of patients eligible for inclusion in the study and the performance of a second cerebrospinal fluid (CSF) sample. Patients were enrolled if they met inclusion criteria for the study.

Eotaxin 12.3-1120, MIP-1β 1.02-750, Eotaxin-3 10.2-3750, TARC 3.32-1120, IP-10 1.37-500, MIP-1α 13.8-743, IL-8713-43400, MCP-1 1.09-375, MDC 88.3-7500, MCP-4 5.13-469, NGF 0.05-498, BDNF 0.72-2000pg/ml, GDNF 2.743-2000, Fractalkine 3.91-250.

2.7. Preparation of the CSF samples for mass spectrometry

A shotgun proteomics approach was employed to analyse the CSF proteome, utilising a single-pot solid-phase-enhanced sample preparation (SP3) for sample preparation (Hughes et al., 2014). The SP3 protocol utilizes commercially available beads which carry a carboxylate moiety. For this experiment both hydrophobic and hydrophilic SeraMag Speed bead Magnetic carboxylate modified particles were employed in a 1:1 mix (GE Healthcare). Prior to use the beads were combined in a ratio of 1:1 (*v*/v), rinsed and reconstituted in MS grade water (Fisher Scientific) at a stock concentration of 10 μg/ml and stored at 4 °C until required.

SP3 preparation was performed according to the protocol of Hughes et al (Hughes et al., 2014). Briefly, 200 μg CSF was resuspended in 100 μl lysis buffer (6 M urea, 2 M thiourea, 50 mM MOPS) and centrifuged for 15 min at 15,000 rpm at 4 °C to remove any cellular debris. The supernatant was transferred to a fresh Eppendorf tube. The CSF was reduced by adding 0.2 M 1,4-dithiothreitol (DTT; Sigma Aldrich) and incubated at 37 °C on a shaker at 700 rpm for 15 min. Samples were then alkylated by adding 0.4 M iodoacetamide (IAA; Sigma Aldrich). Acetonitrile (ACN; Sigma Aldrich) was added to each sample to give a final concentration of 70% acetonitrile (*v*/v) and the prepared SP3 bead mixture was added to each sample and rotated for 18 min at room temperature. Subsequently the beads were immobilized by incubation for 2 min on the DynaMag-2™ stand (Thermo Fisher). The supernatant was discarded and the pellet was rinsed with 70% (v/v) Ethanol in water and 100% ACN. Beads were resuspended in 50 mM ammonium

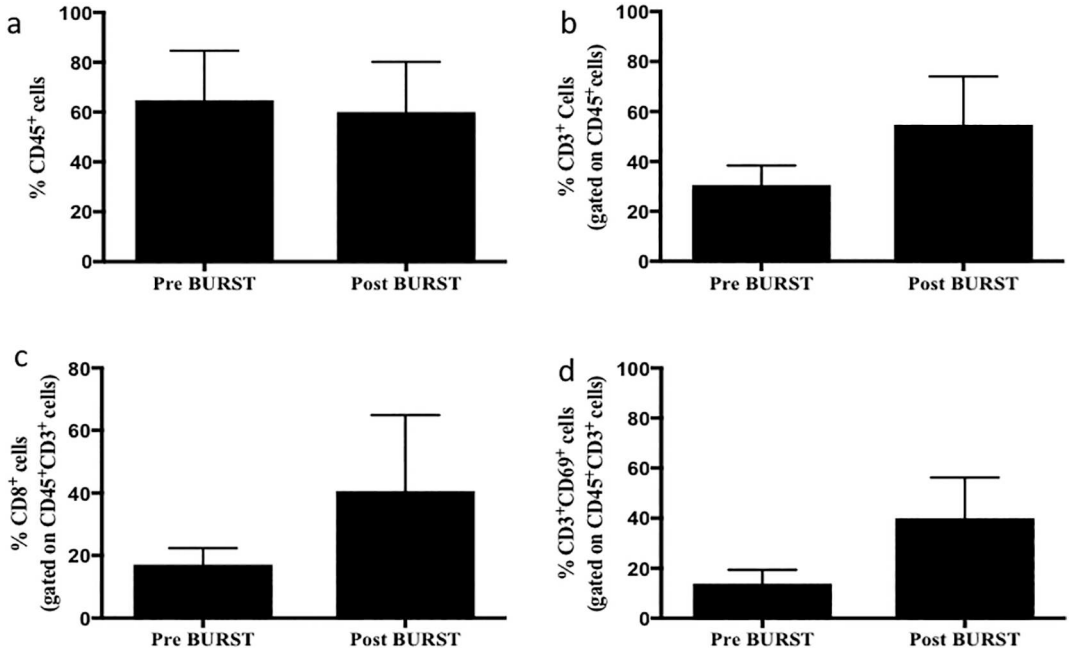

Fig. 3. The percentage frequency of T cells in Cerebrospinal fluid (CSF) before and following 8-weeks after Burst stimulation. Columns indicate the sample means, while the error bars represent the Standard error of the mean (SEM). Statistical analysis was performed using the Mann-Whitney *U* test. Comparison of (a) the percentage of CD45+ cells prior to and following Burst-SCS (64.83% ±19.79 vs 60% ±20.09, $p = .87$), (b) the percentage of CD3+ cells before and after Burst-SCS treatment (30.65% ±7.68 vs 54.73% ±19.29, $p = .25$), (c) the percentage of CD8+ before and after Burst-SCS treatment (17.11% ± 5.27 vs 40.63% ± 24.23, $p = .3179$) and (d) the percentage of CD3+ CD69+ cells before and after Burst-SCS treatment (13.85% ± 5.517 vs 39.97% ±16.31, $p = .1448$).

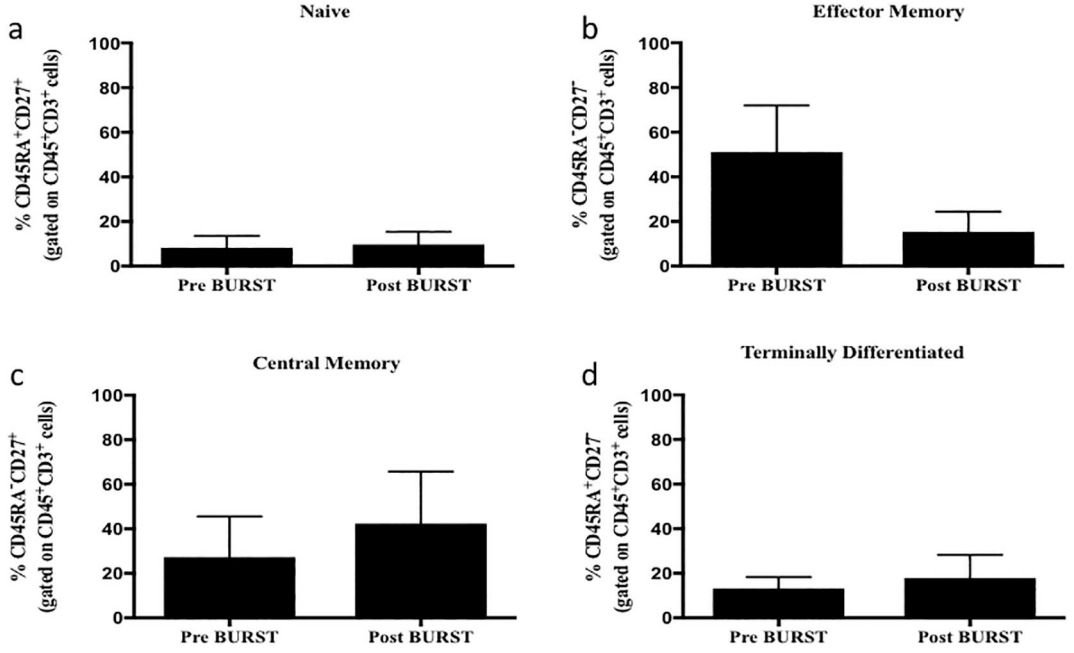

Fig. 4. Phenotype of the percentage of CD8+ cells in the CSF before and following an 8-week duration of Burst stimulation, showing the mean ± standard error of the mean (SEM). Statistical analysis was performed using Mann-Whitney U test. Comparisons of the percentage of (a) Naive cells before and after burst stimulation (8.3% ± 5.22 vs 9.695% ± 5.7, p = .87), (b) Effector Memory cells before and after burst stimulation (51.15% ±20.77 vs 15.35% ±9, $p = .22$), (c) Central memory cells before and after burst stimulation (27.33% ± 18.2 vs 42.33% ±23.4, $p = .62$) and finally (d) terminally differentiated cells before and after burst stimulation (13.23% ±5.07 vs 17.91% ±10.39, $p = .67$).

bicarbonate (NH_4HCO_3; Sigma Aldrich). Lyophilised sequence grade trypsin (Promega) was resuspended in 50 mM ammonium bicarbonate before trypsin was added to each sample. After overnight digestion at 37 °C on a thermoshaker at 500 rpm, prepared bead mixture was added to the samples and ACN was added to reach a final concentration of 95% (v/v). After mixing and incubation, the supernatant was removed and beads were rinsed with 100% ACN. The peptides bound to the beads were eluted using HPLC grade water with intermittent vortexing. The supernatant containing the purified peptides was transferred into a fresh tube containing 10% acetic acid. The samples were placed on the DynaMag-2™ for 5 min before the supernatant was transferred to MS vials for analysis.

Table 3
Pro-Inflammatory Cytokine Panel in Cerebrospinal fluid (CSF) before and 8 weeks after Burst-SCS Stimulation in (pg/ml), $n = 4$.

	Mean baseline +/− SEM (pg/ml)	Mean 8 weeks after burst-SCS +/− SEM (pg/ml)	Mean of differences	SD of differences	SEM of differences	P value Wilcoxon-Sign Rank
IFN-γ	0.1501 ± 0.087	0.1526 ± 0.08826	0.0025	0.1806	0.09	0.99
IL-10	0.1967 ± 0.037	0.2212 ± 0.0278	0.0245	0.0855	0.043	0.625
IL-12p70	0.04869 ± 0.028	0.05026 ± 0.0366	0.0016	0.119	0.0596	1.000
IL-13	2.929 ± 0.5273	1.908 ± 0.6073	−1.022	1.509	0.754	0.375
IL-1β	0.3034 ± 0.086	0.2621 ± 0.05175	−0.041	0.104	0.0522	0.625
IL-4	0.07518 ± 0.027	0.06708 ± 0.0073	−0.0081	0.044	0.022	0.875
IL-6	0.9359 ± 0.159	1.099 ± 0.1141	0.1631	0.134	0.067	0.250
IL-8	21.26 ± 7.367	24.22 ± 4.419	2.958	10.91	5.455	0.625
TNF-α	0.381 ± 0.0339	0.3117 ± 0.0696	−0.069	0.158	0.0794	0.625

Table 4
Cytokine Panel in CSF before and after Burst-SCS Stimulation in (ng/ml), n = 4.

	Mean baseline +/− SEM (pg/ml)	Mean 8 weeks after Burst-SCS +/− SEM (pg/ml)	Mean of differences	SD of differences	SEM of differences	P value Wilcoxon-Sign Rank
IL-12/IL-23p40	3.123 ± 0.3642	3.767 ± 0.2125	0.644	0.470	0.235	0.125
IL-15	3.561 ± 0.5049	3.989 ± 0.4214	0.428	0.565	0.283	0.250
IL-16	8.004 ± 1.322	7.883 ± 1.678	−0.121	1.324	0.662	0.875
IL-17A	0.3253 ± 0.07274	0.4078 ± 0.06008	0.0826	0.1441	0.072	0.375
IL-5	0.5925 ± 0.1123	0.6804 ± 0.1104	0.0879	0.0913	0.045	0.250
IL-7	1.115 ± 0.1406	1.273 ± 0.2115	0.158	0.2193	0.109	0.250
VEGF	2.816 ± 1.414	4.129 ± 1.163	1.313	2.096	1.048	0.50

Table 5
Chemokine Panel in CSF before and after Burst-SCS Stimulation in (ng/ml), n = 4.

	Mean baseline +/− SEM (pg/ml)	Mean 8 weeks after Burst-SCS +/− SEM (pg/ml)	Mean of differences	SD of differences	SEM of differences	P value Wilcoxon-Sign Rank
MCP-1	417.5 ± 55.8	411.9 ± 34.62	−5.64	68.53	34.27	0.875
MCP-4	9.36 ± 1.681	12.56 ± 2.845	3.198	7.548	3.774	0.625
Eotaxin-3	7.731 ± 4.164	20.79 ± 6.781	13.06	9.793	4.896	0.250
Eotaxin	14.99 ± 2.7	17.53 ± 4.09	2.544	5.583	2.792	0.625
MIP-1α	6.41 ± 1.526	7.366 ± 1.406	0.956	2.658	1.329	0.686
MIP-1β	10.45 ± 2.891	9.862 ± 2.089	−0.5911	3.275	1.637	0.625
MDC	40.43 ± 10.05	52.09 ± 17.61	11.66	30.9	15.45	0.625
TARC	6.893 ± 0.5208	7.445 ± 0.5938	0.5523	1.404	0.7019	0.375
Fractalkine	9.402 ± 7.862	4.758 ± 2.064	−4.644	12.62	6.311	0.875
IP-10	129.8 ± 21.55	189.3 ± 53.5	59.56	92.19	46.09	0.375

2.8. LC-MS/MS analysis

Each sample was run in duplicate on a Thermo Scientific Q Exactive mass spectrometer connected to a Dionex Ultimate 3000 (RSLCnano) chromatography system. Each sample was loaded onto a fused silica emitter (75 μm ID), pulled using a laser puller (Sutter Instruments P2000, Novato, CA, USA), packed with ReprocilPur (Dr Maisch, Ammerbuch-Entringen, Germany) C18 (1.9 μm; 12 cm in length) reverse phase media and were separated by an increasing acetonitrile gradient over 60 min at a flow rate of 250 nL/min direct into a Q-Exactive mass spectrometer. The mass spectrometer was operated in positive ion mode with a capillary temperature of 320 °C, and with a potential of 2300 V applied to the frit. All data was acquired while operating in automatic data dependent switching mode. A high resolution (70,000) MS scan (300–1600 m/z) was performed using the Q Exactive to select the 12 most intense ions prior to MS/MS analysis using high-energy collision dissociation (HCD).

2.9. Protein identification and quantification

Proteins were identified and quantified by MaxLFQ (Cox et al., 2014) by searching with MaxQuant version 1.5 against the *Homo sapiens* reference proteome database which was obtained from Uniprot. LFQ intensities of all technical replicates were averaged and all samples obtained before and after SCS were averaged and expressed as a Log_2 value. The log fold change was calculated as well as a false discovery rate (FDR) and p value. Proteins found to be differentially expressed between groups were subjected to pathway mapping analysis and were distributed into categories according to their cellular component, molecular function, and biological process using Ingenuity Pathway Analysis (IPA) [QIAGEN (Redwood City, CA)] or STRING Database (Version 10.5). STRING (www.string-db.org) was used to generate protein-protein interaction networks, which were then imported into Cytoscape for further editing (Version 3.4.0). The NeuroPep database (islab.info/NeuroPep/) and the neuropeptides database (www.neuropeptides.nl) were employed to identify neuropeptides from mass spectrometry. The Brain RNA-Seq tool (www.brainrnaseq.org) was used to establish what cells produced specific proteins. UniProt was used to assess Gene Otology (GO) biological and molecular functions.

2.10. statistical analysis

All statistical analysis was performed on Prism Graph Pad version 7.0. Non-parametric paired and unpaired tests were used where appropriate, Wilcoxon Sign Rank and Mann Whitney respectively. Data was expressed in means with standard error of means (SEM) and

Table 6
Top 25 proteins upregulated (Log fold change >2, FDR < 0.05) following 8 weeks of Burst-SCS stimulation in order of log fold change.

Protein	Gene	Log fold change	FDR
ATP-dependent zinc metalloprotease YME1L1	YME1L1	23.987	0.0446
Double-stranded RNA-specific editase 1	ADARB1	23.921	0.0362
Proliferation marker protein Ki-67	MKI67	22.088	0.0342
Lipopolysaccharide-binding protein	LBP	21.961	0.0303
C-reactive protein	CRP	21.531	0.0229
COP9 signalosome complex subunit 5	COPS5	21.471	0.0442
Metallothionein	MT3	21.404	0.0148
Immunoglobulin lambda variable 4–60	IGLV4–60	21.072	0.0005
Disintegrin and metalloproteinase domain-containing protein 11	ADAM11	21.003	0.0084
Mitotic spindle assembly checkpoint protein MAD1	MAD1L1	20.887	0.0098
Immunoglobulin lambda variable 5–45	IGLV5–45	20.775	0.0059
Cadherin-5	CDH5	20.555	0.0330
Epithelial discoidin domain-containing receptor 1	DDR1	20.476	0.0373
Kallikrein-7	KLK7	20.342	0.0347
Cartilage oligomeric matrix protein, isoform CRA_b	COMP	20.301	0.0137
Adhesion G protein-coupled receptor B1	ADGRB1	20.133	0.0107
Ephrin-A5	EFNA5	20.081	0.0027
Complement C1q tumor necrosis factor-related protein 5	C1QTNF5	20.074	0.0461
Sia-alpha-2,3-Gal-beta-1,4-GlcNAc-R:alpha 2,8-sialyltransferase	ST8SIA3	20.020	0.0176
Complement factor H-related protein 3	CFHR3	20.017	0.0369
DOMON domain-containing protein FRRS1L	FRRS1L	19.970	0.0478
Adenosine deaminase 2	ADA2	19.958	0.008
Ryanodine receptor 3	RYR3	19.880	0.002
Immunoglobulin heavy variable 1–3	IGHV1–3	19.779	0.005
Immunoglobulin kappa variable 1D-16	IGKV1D-16	19.728	0.021

Table 7
Top 25 proteins downregulated (Log fold change <1, FDR < 0.05) following 8 weeks of Burst-SCS stimulation in order of log fold change.

Protein	Gene	Log fold change	FDR
Growth hormone A1	PRL	−22.893	0.0207
Titin	TTN	−22.532	0.0039
Myoglobin	MB	−22.249	0.0223
Somatostatin	SST	−22.226	0.0355
Alpha-actinin-2	ACTN2	−22.115	0.0128
Tropomyosin alpha-4 chain	TPM4	−22.078	0.0163
Calsyntenin-3	CLSTN3	−22.076	0.0456
Spectrin beta chain	SPTBN4	−21.998	0.0101
A disintegrin and metalloproteinase with thrombospondin motifs 1	ADAMTS1	−21.799	0.0485
V-type proton ATPase subunit S1	ATP6AP1	−21.579	0.0395
Contactin-6	CNTN6	−21.373	0.0493
Hepatocyte growth factor-like protein	MST1	−21.206	0.0136
Protein disulfide-isomerase A3	PDIA3	−20.785	0.0328
Semaphorin-3G	SEMA3G	−20.739	0.0472
Oral-facial-digital syndrome 1 protein	OFD1	−20.623	0.0184
Serotransferrin	TF	−20.473	0.0100
Calnexin	CANX	−20.450	0.0323
WAP four-disulfide core domain protein 2	WFDC2	−20.299	0.0386
Junction plakoglobin	JUP	−20.186	0.0294
Voltage-dependent calcium channel subunit alpha-2/delta-3	CACNA2D3	−20.063	0.0425
CD320 antigen	CD320	−20.049	0.0166
Plexin-B1	PLXNB1	−19.987	0.0175
OX-2 membrane glycoprotein	CD200	−19.980	0.0338
Neuromodulin	GAP43	−19.953	0.0301
Piezo-type mechanosensitive ion channel component	PIEZO2	−19.844	0.01134

standard deviations (SD). *P* values of <0.05 were considered to be significant for the flow-cytometry and ELISA analysis. A separate analysis for the proteomic data is described in section 3.4.

3. Results

3.1. Patient enrolment

In accordance with the exclusion and inclusion criteria a total of 4 patients (2 females, 2 males) participated in the study (Fig. 2), with a mean age of 51 years (+/− SEM 2.74, SD 5.48) shown in the patient demographics (Table 1). The patients respective pain scores and stimulation parameters were documented (Table 2), with all of the patients deemed to be responders following 8 weeks of Burst-SCS (Fig 2). It was also noted that the patients received no changes in medications between the initial CSF sampling and the follow up sampling after 8 weeks of Burst-SCS treatment.

3.2. Cellular analysis

There were no significant differences in the percentage (%) frequencies of T cells in the CSF samples obtained prior to and after stimulation. Some higher frequencies were observed in the $CD3^+$ cells (Pre vs Post Burst-SCS: $CD3^+$ cells: 30.7% ±7.7% vs 54.7% ±19.3%, $p = .25$), $CD8^+$ T cell frequencies (Pre vs Post Burst-SCS $CD8^+$ T cells: 17.1% ± 5.3 vs 40.6% ± 24.2, $p = .3179$) as wells as those of activated ($CD69^+$) T cells (Pre vs Post Burst-SCS $CD69^+CD3^+$ cells: 13.9% ± 5.5% vs 40% ±16.3%, $p = .1448$) (Fig. 3). However, none of these changes were found to be significant. There was a reversal of effector memory (EM)/central memory (CM) T cell phenotype following Burst-SCS stimulation but this was not significant (EM Pre vs Post Burst-SCS: 51.2% ± 20.7% vs 15.4% ± 9%, $p = .2224$) (CM Pre vs Post Burst-SCS: 27.3% ± 18.2% vs 42.3% ± 23.4%, $p = .6281$) (Fig. 4).

3.3. Cytokines, chemokines and neurotrophins analysis

There were no significant differences in the concentrations of a panel of cytokines and chemokines analysed within the CSF before and after stimulation (Tables 3, 4 and 5). The following neuropeptides were undetectable within the CSF at both time-points for all patients; Nerve growth factor (NGF), brain derived neurotrophic factor (BDNF), glial cell derived neurotrophic factor (GDNF), GM-CSF, IP-10, TNF-β and IL-2. All other cytokines were within range according to the manufacturer's instructions.

3.4. Proteomics analysis

To determine the effects on protein expression in the CSF, the proteomics data obtained from patients following 8 weeks of Burst-SCS was compared to CSF obtained from the same patients prior to beginning treatment. In total 992 proteins were identified in the CSF obtained from patients, with differential expression of proteins observed in samples obtained prior to and after Burst-SCS stimulation. For the purposes of identifying proteins which were significantly altered following Burst-SCS strict filtering settings were applied to the proteomics data in order identify proteins which were significantly increased (log fold change (LFC) > 2, FDR < 0.05) (Table 6) and decreased (LFC <1, FDR <0.05) (Table 7) following Burst-SCS stimulation.

Compared to CSF obtained prior to treatment, CSF obtained following an 8-week course of Burst-SCS resulted in the differential expression of 477 proteins (48.1% of total proteins; FDR < 0.05) (Fig. 5a). Of these 477 differentially expressed proteins, 346 proteins were upregulated (72.5%) and 131 proteins were downregulated (27.5%) following Burst-SCS (−2 < LFC > 2) (Fig. 5a). Focusing on these differentially expressed proteins a total of 38 proteins (8%) were

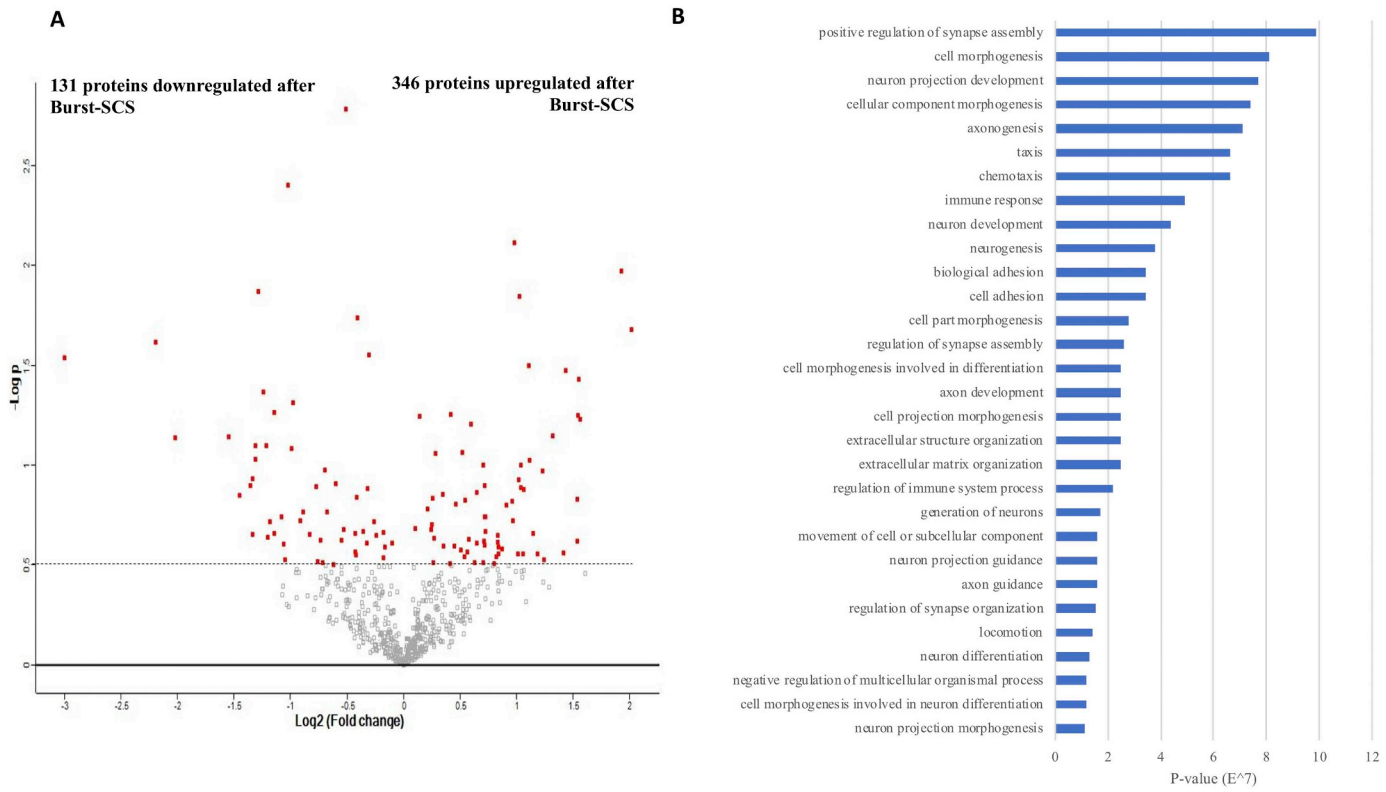

Fig. 5. Differential protein expression in Cerebrospinal Fluid (CSF) obtained prior to treatment and following an 8-week course of Burst-SCS: Volcano plot showing protein differential data of the 648 proteins differentially expressed (5A). Of the differentially expressed proteins, 346 proteins were upregulated (53.4%) and 131 proteins were downregulated (20.2%). The significant differentiated proteins are in red: 38 proteins (4.8%) were significantly upregulated and 42 (6.5%) were downregulated after Burst-SCS (Fig. 5a). GO biological functional enrichment analysis of 30 biological processes involving the differentially expressed proteins (5B). The top 5 biological processes identified as the positive regulation of synapse assembly ($p < 9.9E^{-7}$), cell morphogenesis ($p < 8.1E^{-7}$), neuron projection development ($p < 7.7E^{-7}$), cellular component morphogenesis ($p < 7.4E^{-7}$) and axonogenesis ($p < 7.1E^{-7}$). (For interpretation of the references to colour in this figure legend, the reader is referred to the web version of this article.)

shown to be significantly upregulated while 42 proteins (8.8%) were shown to be significantly downregulated after Burst-SCS (FDR < 0.05) (Fig. 5a).

GO analysis focusing on the biological functional enrichment identified 30 biological processes involving the differentially expressed proteins, with the top 5 biological processes identified as the positive regulation of synapse assembly ($p < 9.9E^{-7}$), cell morphogenesis ($p < 8.1E^{-7}$), neuron projection development ($p < 7.7E^{-7}$), cellular component morphogenesis ($p < 7.4E^{-7}$) and axonogenesis ($p < 7.1E^{-7}$). Focusing on the 477 differentially expressed proteins, the proteins could be classified into protein classes (i.e., transporters, enzymes (including kinases and peptidases), receptors (including G protein coupled receptors, transmembrane receptors and ion channels), and immune effectors) as defined by International Union of Basic and Clinical Pharmacology (Fig. 6a, b).

Further analysis focusing on the differentially expressed proteins identified a cohort of 24 known neuropeptides which demonstrated differential analysis following treatment, with the expression of 8 of these identified neuropeptides shown to be significantly changed following treatment (FDR < 0.05) (Fig. 7). Seven neuropeptides were shown to be increased following Burst-SCS, including proenkephalin-A (PENK), cerebellin-3 (CBLN3), cocaine and amphetamine-regulated transcript protein (CARTPT), nucleobindin-1 (NUCB1), kininogen-1 (KNG1), cerebellin-1 (CBLN1) and angiotensinogen (AGT), but the changes were found to be nonsignificant when stricter filtering was applied (Log fold change > 1, FDR < 0.05) (Table 8). In addition, 18 neuropeptides were shown to be decreased following Burst-SCS treatment (Table 9). Neuropeptides demonstrating significant decreases in expression following burst SCS include growth hormone A1 (PRL), somatostatin (SST), nucleobindin-2 (NUCB2), Calbindin (CALB1), acyl-CoA binding protein (DBI), proSAAS (PCSK1N), endothelin-3 (END3) and cholecystokinin (CCK) (Table 9). The GO molecular function and biological processes for each of these significantly altered proteins was assessed (Table 10).

4. Discussion

We present the results of a pilot study examining the effect of Burst-SCS on the cellular and neuropeptide constituents of CSF in patient responders with neuropathic pain. All of the patients recruited were responders (>50% pain relief) to Burst-SCS in order to give an accurate analysis of the treatment response. This is the first molecular description of the effect of Burst-SCS on CSF constituents in vivo potentially validating its ability to target the neural interface in the CNS.

The development of Burst-SCS was based upon information regarding thalamo-cortical firing patterns having the ability to strengthen synaptic connectivity (Krahe and Gabbiani, 2004; Sherman, 2001; Swadlow and Gusev, 2001). The majority of proteins differentiated after Burst-SCS illustrate a modulation in relation to synapse assembly using biological enrichment analysis. Synapse assembly is largely orchestrated by glial cells within the CNS which includes astrocytes (Chung et al., 2015; Ullian et al., 2004) and microglia (Kettenmann et al., 2013; Salter and Beggs, 2014). Long term synaptic changes have been previously demonstrated with bursts of stimulation in the hippocampus in rats (Remy and Spruston, 2007). There is also pre-clinical evidence of BNF being transmitted across synapses more reliably which may be indicative of this alteration in neuronal physiology (Krahe and Gabbiani, 2004). It is difficult to determine the exact processes of this

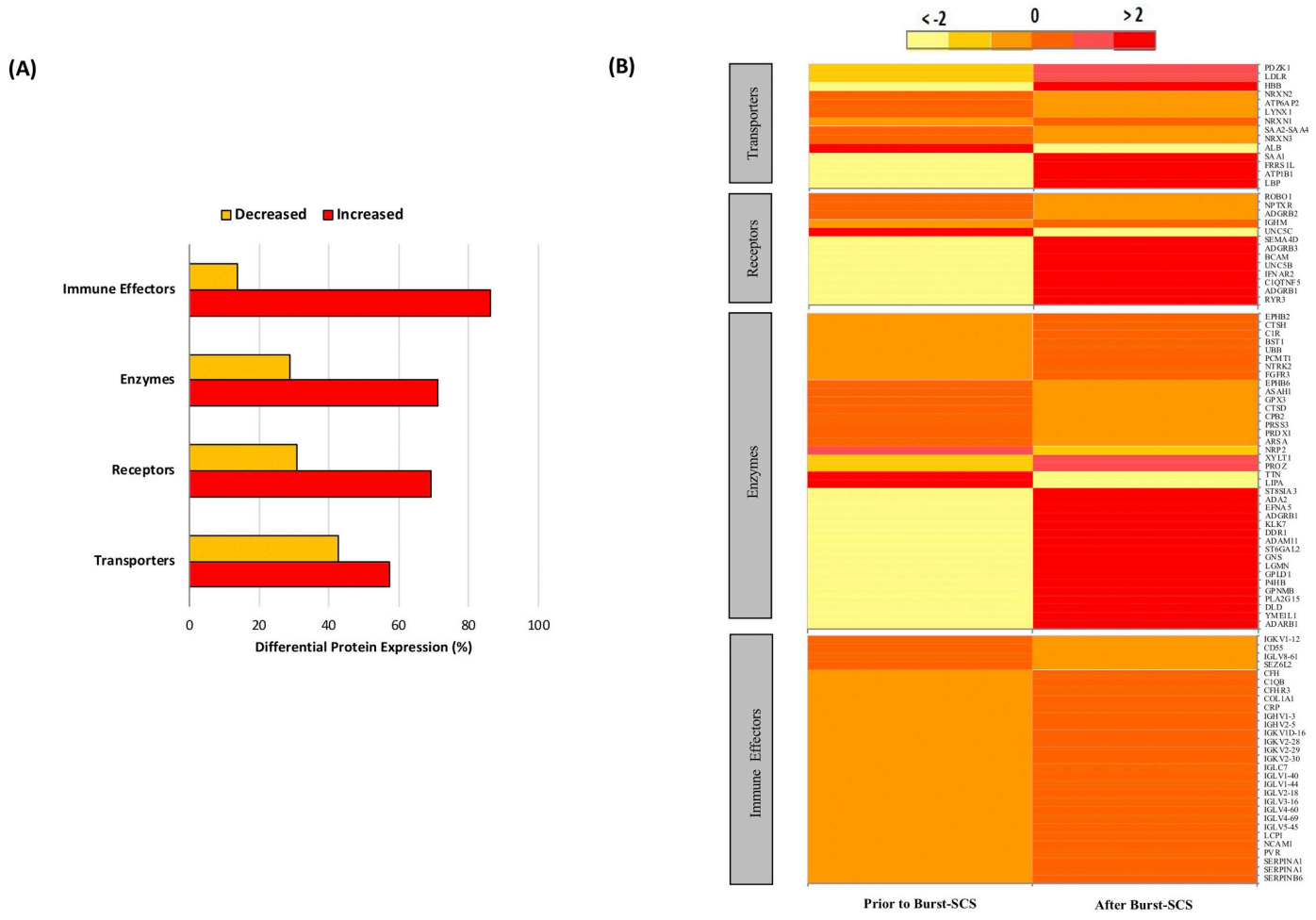

Fig. 6. Bar chart showing classification of % of differentially expressed protein classes as defined by International Union of Basic and Clinical Pharmacology (6A): transporters, enzymes (including kinases and peptidases), receptors (including G protein coupled receptors, transmembrane receptors and ion channels), and immune effectors. Relative expression of each protein (gene class) in a bar plot, red representing upregulation and yellow downregulation (6B). (For interpretation of the references to colour in this figure legend, the reader is referred to the web version of this article.)

alteration from the enrichment analysis however. In terms of protein classes, immune effectors were the predominant increased neuropeptides. Immune mediators including pro-inflammatory cytokines also have significant effects on neurotransmission at the synaptic cleft which is frequently referred to as the 'neuroimmune interface' (Grace et al., 2014). Despite proteomic evidence in the change of immune effectors, no significant differences were identified in the frequency of T cells, or the concentrations of secreted cytokines or chemokines within the CSF before and after 8 weeks of Burst-SCS in this study. There was however a modest, non-significant increase in the percentage of $CD8^+$ T cells which may be related to the increase in immune effectors. Interestingly, the predominant T cell memory phenotype was effector memory prior to stimulation, which is in line with our group's previous report of a series of patients with lumbar radicular neuropathic pain prior to any treatment (Das et al., 2018). This is in contrast to T cell populations within the CSF of healthy controls which are predominantly central memory (de Graaf et al., 2011a; de Graaf et al., 2011b). Pre-clinical studies have frequently implicated T cells in the development, maintenance and resolution of neuropathic pain (Austin et al., 2012; Costigan et al., 2009; Duffy et al., 2018; Krukowski et al., 2016; Luchting et al., 2015; Sorge et al., 2015; Tang et al., 2013; Totsch and Sorge, 2017; Yang et al., 2018). Immune related peptides have also been the most upregulated in spinal cord segments analysed after sciatic nerve ligation in a study in rodents following tonic SCS (Stephens et al., 2018). The same study also illustrated key transcriptional pathways induced by SCS including decreased efficacy of synaptic signalling mediated via genes that encode scaffold proteins (Stephens, Chen, 2018).

Proteomic analysis revealed that growth hormone A1 (PRL) and somatostatin (SST) demonstrated significantly lower expression following Burst-SCS. Growth hormone (GH) signalling molecules have been implicated in nociception and the development of neuropathic pain (Xu et al., 2019). There is also selective evidence of growth hormone reducing neuropathic pain in cases of fibromyalgia and reversing pain behaviour in rodents (Xu et al., 2019). This would appear contradictory to our findings. SST, an inhibitor of GH release was also significantly lower after Burst-SCS. There are conflicting reports of how SST modulates both pain and pruritis in pre-clinical models with evidence of both attenuation and causative (Carlton et al., 2001; Carlton et al., 2004; Chapman and Dickenson, 1992; Huang et al., 2018; Seybold et al., 1982; Shi et al., 2014; Wiesenfeld-Hallin, 1985). NUCB2 was significantly lower following Burst-SCS and this protein is known to have a role in hypothalamic pathways and endocrine function but is potentially expressed by multiple cells within the CNS (Tagaya et al., 2012). Given PRL, SST and NUCB2 are involved in hypothalamic functions it may be indicative of supraspinal mechanisms when applying Burst-SCS to the spinal cord. However, the attenuated release of these neuropeptides may occur at a more caudal location in the spinal cord. Despite this uncertainty, a neurophysiological study in humans using fluorodeoxyglucose positron emission tomography (FGD-PET)

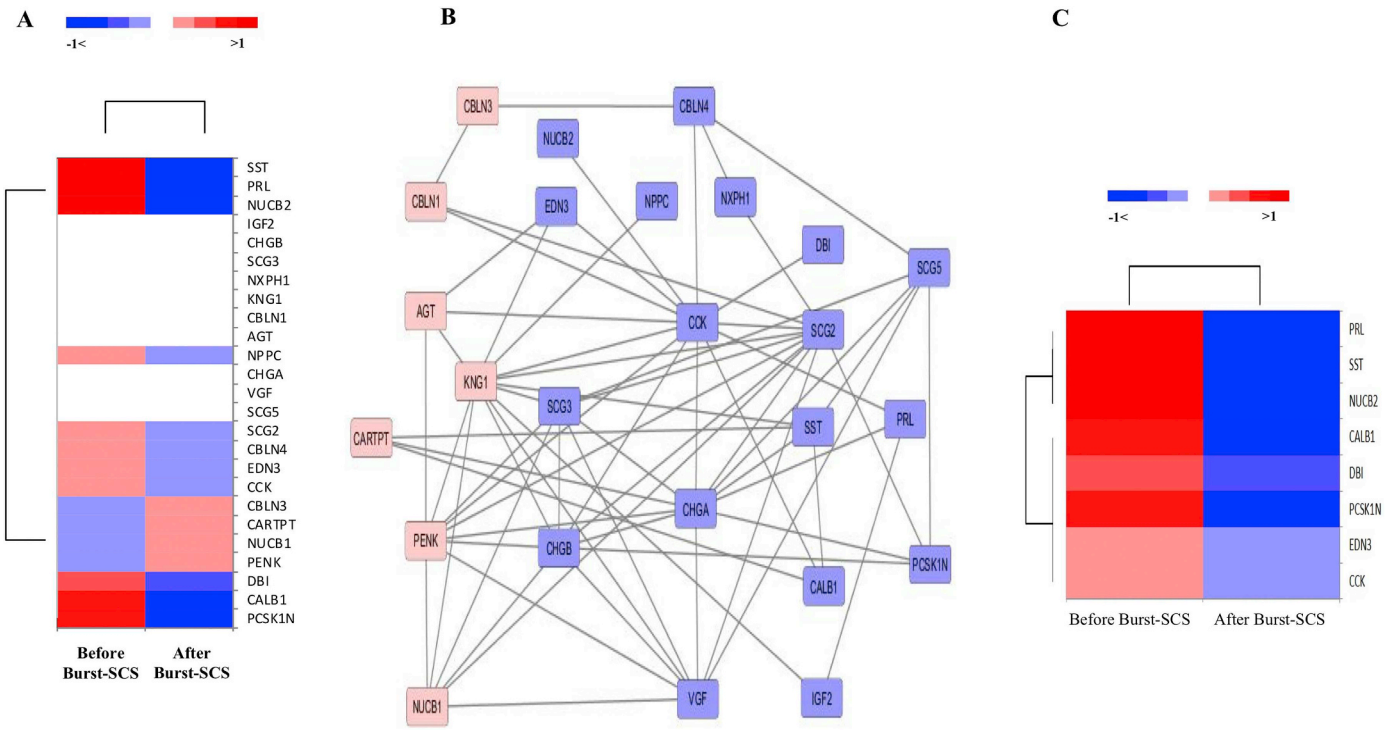

Fig. 7. Differential expression of neuropeptides after Burst-SCS. A shows the differential expression of 24 neuropeptides. B shows the neuropeptide network, with neuropeptides showing increased expression after Burst-SCS shown in blue while neuropeptides showing decreased expression after treatment are shown in pink. C shows a heatmap with the expression of 8 of these identified neuropeptides shown to be significantly changed following treatment (FDR < 0.05). FDR = false discovery rate. (For interpretation of the references to colour in this figure legend, the reader is referred to the web version of this article.)

Table 8
Proteomic Mass spectrometry: Neuropeptides increased (Log fold change >0, False discovery rate (FDR) <0.05) in CSF following 8 weeks of Burst-SCS Stimulation. The Brain RNA-Seq tool (www.brainrnaseq.org) was used to establish what cells produced specific proteins. Proteins which were significantly decreased (Log fold change>1, FDR < 0.05) are denoted by an asterix.

Protein	Gene	Cells that produce in CNS	Log fold change	FDR
Proenkephalin-A	PENK	Neurons, Oligodendrocytes Endothelial	0.8554	0.0206
Cerebellin-3	CBLN3	Neurons	0.5484	0.0410
Cocaine- and amphetamine-regulated transcript protein	CARTPT	Astrocytes, Endothelial	0.5464	0.03961
Nucleobindin-1	NUCB1	Astrocytes, Endothelial, Microglia, Oligodendrocytes, Neurons	0.3729	0.0368
Kininogen-1	KNG1	Neurons	0.1052	0.0206
Cerebellin-1	CBLN1	Neurons, Oligodendrocytes	0.0918	0.0315
Angiotensinogen	AGT	Astrocytes, Neurons,	0.0331	0.020

scanning illustrated activation of the corticolimbic system via the dorsal anterior cingulate cortex with Burst-SCS (Yearwood, De Ridder, 2019). Similar results were also achieved with electroencephalography (EEG) (De Ridder and Vanneste, 2016) in patients with Burst-SCS. It must be noted that both of these studies had low numbers of participants and did not illustrate modulation of the hypothalamic-pituitary axis (De Ridder and Vanneste, 2016; Yearwood, De Ridder, 2019). The corticolimbic system, which includes the hypothalamic pituitary axis, is strongly associated with emotional components of chronic pain and depression (Blackburn-Munro, 2004; Vachon-Presseau, 2018). The hypothalamic-pituitary axis may also have the potential to restore metabolic associated pathological neural transmission and chronic pain in the periphery (Kinfe et al., 2019). Somatostatin receptors are present on immune cells and can have an effect on the release of cytokines which can modulate pain transmission (Backonja et al., 2008; Cook et al., 2018; Hung et al., 2017; ten Bokum et al., 2000; Zhang and An, 2007). Changes to metabolic and immune associated peptides in serum have previously been reported in responders to Burst-SCS (Muhammad et al., 2018). These included leptin, indicating central mechanisms can alter differential cytokine/adipokine traffic peripherally; however only the cytokine IL-10 was significantly altered (Muhammad, Chaudhry, 2018). Pre-clinical evidence supports the role of ProSAAS in the control of the neuroendocrine secretory pathway (Mzhavia et al., 2001; Mzhavia et al., 2002). ProSAAS was also significantly lower after Burst-SCS and has previously been significantly upregulated in the CSF of patients with fibromyalgia compared to healthy controls (Khoonsari et al., 2019a). Given these two findings the role of ProSAAS in chronic neuropathic pain justifies further clinical research.

Calbindin (CALB1) is a calcium binding protein that is involved in many biological processes within the CNS including synaptic plasticity but there is little evidence to date that it has an effect on pain processing (Berg et al., 2018; Ren and Ruda, 1994; Schwaller et al., 2002). Burst-SCS is thought to ride on a calcium mediated plateau and NUCB2 also binds calcium and is involved in calcium homeostasis (Chakravarthy et al., 2019). As peripheral neuropathies and chronic pain have implicated calcium dysregulation in their pathologies modulating calcium homeostasis may have positive effects for pain perception (Fernyhough and Calcutt, 2010; Hagenston and Simonetti, 2014; Mei et al., 2018; Navarrete et al., 2013; Perea and Araque, 2005).

Diazepam binding protein (DBI) is classified as an acyl-CoA binding domain containing proteins (ABCD1) that regulates mitochondrial Translocator protein (TSPO) function and is largely expressed in glial

Table 9
Proteomic Mass spectrometry: Neuropeptides decreased (Log fold change <0, False discovery rate (FDR) <0.05) in CSF following 8 weeks of Burst-SCS Stimulation. The Brain RNA-Seq tool (www.brainrnaseq.org) was used to establish what cells produced specific proteins. Proteins which were significantly decreased (Log fold change <-1, FDR <0.05) are denoted by an Asterix.

Protein	Gene	Cells that produce in CNS	Log fold change	FDR
Growth hormone A1	PRL	Neurons	−22.893	0.0207*
Somatostatin	SST	Neurons, Oligodendrocytes, Endothelial, Astrocytes	−22.226	0.0355*
Nucleobindin-2	NUCB2	Neurons, astrocytes, Oligodendrocytes, Endothelial, Microglia	−18.750	0.0012*
ProSAAS	PCSK1N	Oligodendrocytes	−1.863	0.0484*
Calbindin	CALB1	Neurons, Astrocytes, Endothelial	−1.551	0.0251*
Acyl-CoA-binding protein	DBI	Microglia, Astrocytes, Oligodendrocytes, Neurons, Endothelial	−1.242	0.0038*
Cholecystokinin	CCK	Neurons, Mature Astrocytes, Oligodendrocytes, Endothelial	−0.7368	0.0252
Endothelin-3	EDN3	Endothelial	−0.588	0.0291
Cerebellin-4	CBLN4	Neurons	−0.495	0.0473
Secretogranin-2	SCG2	Neurons, Oligodendrocytes, Astrocytes, Endothelial	−0.491	0.0288
C-type natriuretic peptide	NPPC	Astrocytes, Neurons	−0.325	0.0317
Chromogranin-A	CHGA	Neurons	−0.273	0.0281
Neurosecretory protein VGF	VGF	Neurons	−0.224	0.0174
Neuroendocrine protein 7B2	SCG5	Neurons, Oligodendrocytes, Endothelial, Astrocytes, Microglia	−0.212	0.0248
Neurexophilin-1	NXPH1	Neurons, Oligodendrocytes, Astrocytes, Endothelial	−0.120	0.009
Secretogranin-3	SCG3	Astrocytes, Neurons, Oligodendrocytes, Endothelial	−0.115	0.0435
Secretogranin-1	CHGB	Neurons, Oligodendrocytes, Endothelial, Astrocytes, Microglia	−0.0766	0.0245
Insulin-like growth factor II	IGF2	Endothelial	−0.046	0.0207

Table 10
GO Molecular, Biological function and immune activity of proteins downregulated with Burst SCS.

Protein	Gene	GO- Molecular Function	GO- Biological process
Growth hormone A1	PRL	Hormone activity	Involved in the prolactin signalling pathway as a positive regulator, Hyperosmotic response, chemical synaptic transmission
Somatostatin	SST	Hormone activity	Involved in the somatostatin signalling pathway, locomotor activity,cognitive function, chemical synaptic transmission
Nucleobindin-2	NUCB2	DNA and Calcium ion binding	Negative regulation of appetite
ProSAAS	PCSK1N	Signalling receptor binding	Neuropeptide signalling pathway, peptide hormone processing, response to cold and dietary excess
Calbindin	CALB1	Calcium ion binding (involved in regulation of pre and postsynaptic cytosolic calcium ion concentration) Vitamin D and Zinc binding	Regulation of long term synaptic potential, short and long term memory, locomotory behaviour, retina layer formation, cochlea development
Acyl-CoA-binding protein	DBI	Benzodiazepine receptor, lipid, long-chain fatty acyl-CoA binding, protein dimerization acitivity	Acyl-CoA metabolic process, phosphatidylcholine acyl-chain remodelling
Cholecystokinin	CCK	Hormone activity	Axonogensis, memory, signal transduction, positive regulation of sensory perception of pain,negative regulation of appetite, positive regulation of fear response, positive regulation of glutamate response
Endothelin-3	END3	Endothelin B receptor binding, hormone activity, signal receptor binding	Blood circulation, cellular calcium and magnesium ion homeostasis, neuron differentiation, signal transduction, immune chemotaxis, positive regulation of hormone secretion

cells in the CNS (Rupprecht et al., 2010). TSPO is a protein expressed in steroid synthesising cells and is involved in the translocation of cholesterol from the outer to the inner mitochondrial membrane (Rupprecht et al., 2010). It is utilised as a marker of brain and spinal cord inflammation and is involved in autocrine and paracrine signalling responses in glial cells to disease (Albrecht et al., 2018a; Albrecht et al., 2018b; Loggia et al., 2015; Rupprecht et al., 2010). Radiolabelled TSPO is upregulated in the CNS in many chronic pain patients compared to controls with chronic back pain (Albrecht et al., 2018b; Loggia et al., 2015), Complex Regional Pain Syndrome (CRPS)(Jeon et al., 2017), fibromyalgia (Albrecht et al., 2018b) and lumbar radicular pain (Albrecht et al., 2018a). As DBI was lower following Burst-SCS in our cohort, this potentially indicates a reduction in neuroinflammation in glial cells.

CCK was significantly lower after Burst-SCS and has previously been implicated in the chronicity of neuropathic pain and reducing the anti-nociceptive effect of opioids (Hebb et al., 2005; Rowlingson, 2007). Increased CCK levels have also been associate with motivational loss, anxiety and panic attacks that are frequently seen in chronic pain patients (Hebb et al., 2005). CCK's reduction may also contribute to the analgesic and psychological improvement observed with Burst-SCS (Kirketeig et al., 2019).

Endothelin-3 (EDN3) (lower expression after Burst-SCS) is part of the endothelin family that have been heavily implicated in many chronic and acute pain conditions (Khodorova et al., 2009; Smith et al., 2014). The majority of research has been performed with EDN1, however EDN3 is known to bind to the same receptors as EDN1. EDN3 is more associated as an agonist to the ET-B receptor which it has a 100-fold higher affinity in comparison to the ET-A receptor. ET-B receptors are upregulated in a sciatic nerve ligation models and antagonism is associated with a reduction of allodynia in pre-clinical models of trigeminal neuralgia (Smith et al., 2014). The role of EDN3 and the ET-B receptor requires more attention in future clinical and pre-clinical research. There is an isolated case report of a patient with sciatica reporting a reduction in pain after administration of a endothelin-A antagonist for pulmonary hypertension (Murphy et al., 2010). However, to date, there have been no further reports or studies relating to EDN3 and neuropathic pain in humans.

A major limitation of this observational study is the small number of patients and the findings therefore require validation in a larger cohort. Although pathologies were different, patients with the same pathology of neuropathic pain often present with different symptoms and phenotyping in any study remains a challenge (van Hecke et al., 2015). What is more important is that all of the patients in this study

responded to Burst-SCS. The phenotyping of patients to different waveforms of SCS has yet to be addressed in clinical studies. There is also little evidence to profile and phenotype CSF constituents between different patients with neuropathic pain and is largely confined to individual studies using controls (Bjurstrom et al., 2016; Khoonsari et al., 2019b). Participants also had CSF taken at different distances to the target therapy, but other proteomic studies have highlighted that rostral-caudal gradient of CNS proteins does not differ along the axis of the spine (Aasebo et al., 2014; Lind et al., 2016). Some studies using CSF routinely check for contamination by assessing the number of red cells within the sample (de Graaf et al., 2011a; de Graaf et al., 2011b; Hummert et al., 2018; Maxeiner et al., 2009; Subira et al., 2002). While we did not perform this check the application of a fine gauge needle which was utilised in our study led to minimal contamination in other studies (de Graaf et al., 2011a; de Graaf et al., 2011b). Even in the presence of blood contamination protein level changes within the CNS have been successfully measured but this needs to be taken into account (Aasebo et al., 2014). None of the proteins significantly differentially expressed were related to possible blood contamination (Aasebo et al., 2014). Although there were no controls in this study, variations in repeated samples in the same individual do not demonstrate significant variation for proteomic analysis (Schutzer et al., 2010). Despite this a control group of non-responders to Burst-SCS would provide a stronger analysis. It would also be useful in future studies to use patient-matched blood samples for comparison or to include a sham control group to differentiate from potential placebo responders.

5. Conclusion

Our research in this pilot study provides the first indication that the CSF proteome is altered by Burst-SCS. However, due to the small sample size any results should be considered preliminary in nature. The differential pathways altered in our cohort include those involved in synapse assembly and immune regulation. Significantly lower levels of singular proteins also suggest supraspinal and potential neuroendocrine effects. The ability of Burst-SCS to alter pathways in multiple cells within the CNS suggests that the mechanism of action is not solely dependent upon selective neuronal discharge. More research into the effect of Burst-SCS on CNS cellular function is required to fully elucidate its mechanism of action. We propose that a combination of multiple diagnostic and physiological parameters should be scrutinized to advance our knowledge of Burst-SCS's effects and the pathophysiology of chronic neuropathic pain.

Funding

The study was funded by a research grant from the College of Anaesthesiologists of Ireland (Research Grant 2016). The funding source had no role in design; collection, analysis and interpretation of data; in the writing of the article and the decision to submit the article for publication.

Author contributions

JR, MC, JL, CM: Conceptualized, Methodology. JR, CM: Investigation. JR, MC, MD, HC, DM: Formal analysis, Validation, Data Curation. JR Writing- Original Draft. All authors contributed to the manuscript and reviewed prior to submission.

Declaration of Competing Interest

None.

Acknowledgements

The authors would like to thank Dr. Joseph Fitzgerald and Dr. Basabjit Das for helping to recruit patients for this study.

References

Aasebo, E., Opsahl, J.A., Bjorlykke, Y., Myhr, K.M., Kroksveen, A.C., Berven, F.S., 2014. Effects of blood contamination and the rostro-caudal gradient on the human cerebrospinal fluid proteome. PLoS One 9, e90429.
Ahmed, S., Yearwood, T., De Ridder, D., Vanneste, S., 2018. Burst and high frequency stimulation: underlying mechanism of action. Expert Rev. Med. Devices. 15, 61–70.
Albrecht, D.S., Ahmed, S.U., Kettner, N.W., Borra, R.J.H., Cohen-Adad, J., Deng, H., et al., 2018a. Neuroinflammation of the spinal cord and nerve roots in chronic radicular pain patients. Pain. 159, 968–977.
Albrecht, D.S., Normandin, M.D., Shcherbinin, S., Wooten, D.W., Schwarz, A.J., Zurcher, N.R., et al., 2018b. Pseudoreference regions for glial imaging with (11)C-PBR28: investigation in 2 clinical cohorts. J. Nucl. Med. 59, 107–114.
Association of Anaesthetists of Great B, Ireland, Obstetric Anaesthetists A, Regional Anaesthesia UK, Association of Paediatric Anaesthetists of Great B, Ireland, et al, 2014. Safety guideline: skin antisepsis for central neuraxial blockade. Anaesthesia 69, 1279–1286.
Austin, P.J., Kim, C.F., Perera, C.J., Moalem-Taylor, G., 2012. Regulatory T cells attenuate neuropathic pain following peripheral nerve injury and experimental autoimmune neuritis. Pain. 153, 1916–1931.
Backonja, M.M., Coe, C.L., Muller, D.A., Schell, K., 2008. Altered cytokine levels in the blood and cerebrospinal fluid of chronic pain patients. J. Neuroimmunol. 195, 157–163.
Berg, E.M., Bertuzzi, M., Ampatzis, K., 2018. Complementary expression of calcium binding proteins delineates the functional organization of the locomotor network. Brain Struct. Funct. 223, 2181–2196.
Bjurstrom, M.F., Giron, S.E., Griffis, C.A., 2016. Cerebrospinal fluid cytokines and neurotrophic factors in human chronic pain populations: a comprehensive review. Pain Pract. 16, 183–203.
Blackburn-Munro, G., 2004. Hypothalamo-pituitary-adrenal axis dysfunction as a contributory factor to chronic pain and depression. Curr. Pain Headache Rep. 8, 116–124.
Bocci, T., De Carolis, G., Paroli, M., Barloscio, D., Parenti, L., Tollapi, L., et al., 2018. Neurophysiological comparison among tonic, high frequency, and burst spinal cord stimulation: novel insights into spinal and brain mechanisms of action. Neuromodulation: Technology at the Neural Interface 21, 480–488.
Bouhassira, D., Attal, N., Alchaar, H., Boureau, F., Brochet, B., Bruxelle, J., et al., 2005. Comparison of pain syndromes associated with nervous or somatic lesions and development of a new neuropathic pain diagnostic questionnaire (DN4). Pain. 114, 29–36.
Cacace, F., Mineo, D., Viscomi, M.T., Latagliata, E.C., Mancini, M., Sasso, V., et al., 2017. Intermittent theta-burst stimulation rescues dopamine-dependent corticostriatal synaptic plasticity and motor behavior in experimental parkinsonism: possible role of glial activity. Mov. Disord. 32, 1035–1046.
Carlton, S.M., Du, J., Zhou, S., Coggeshall, R.E., 2001. Tonic control of peripheral cutaneous nociceptors by somatostatin receptors. J. Neurosci. 21, 4042–4049.
Carlton, S.M., Zhou, S., Du, J., Hargett, G.L., Ji, G., Coggeshall, R.E., 2004. Somatostatin modulates the transient receptor potential vanilloid 1 (TRPV1) ion channel. Pain. 110, 616–627.
Caylor, J., Reddy, R., Yin, S., Cui, C., Huang, M., Huang, C., et al., 2019. Spinal cord stimulation in chronic pain: evidence and theory for mechanisms of action. Bioelectronic Med. 5.
Chakravarthy, K., Kent, A.R., Raza, A., Xing, F., Kinfe, T.M., 2018. Burst spinal cord stimulation: review of preclinical studies and comments on clinical outcomes. Neuromodulation. 21, 431–439.
Chakravarthy, K., Fishman, M.A., Zuidema, X., Hunter, C.W., Levy, R., 2019. Mechanism of action in burst spinal cord stimulation: review and recent advances. Pain Med. 20, S13–S22.
Chapman, V., Dickenson, A., 1992. The effects of sandostatin and somatostatin on nociceptive transmission in the dorsal horn of the rat spinal cord. Neuropeptides. 23, 147–152.
Chung, W.-S., Allen, N.J., Eroglu, C., 2015. Astrocytes control synapse formation, function, and elimination. Cold Spring Harb. Perspect. Biol. 7, a020370.
Colloca, L., Ludman, T., Bouhassira, D., Baron, R., Dickenson, A.H., Yarnitsky, D., et al., 2017. Neuropathic pain. Nat. Rev. Dis. Primers. 3, 17002.
Cook, A.D., Christensen, A.D., Tewari, D., McMahon, S.B., Hamilton, J.A., 2018. Immune cytokines and their receptors in inflammatory pain. Trends Immunol. 39, 240–255.
Costigan, M., Moss, A., Latremoliere, A., Johnston, C., Verma-Gandhu, M., Herbert, T.A., et al., 2009. T-cell infiltration and signaling in the adult dorsal spinal cord is a major contributor to neuropathic pain-like hypersensitivity. J. Neurosci. 29, 14415–14422.
Courtney, P., Espinet, A., Mitchell, B., Russo, M., Muir, A., Verrills, P., et al., 2015. Improved pain relief with burst spinal cord stimulation for two weeks in patients using tonic stimulation: results from a small clinical study. Neuromodulation. 18, 361–366.
Cox, J., Hein, M.Y., Luber, C.A., Paron, I., Nagaraj, N., Mann, M., 2014. MaxLFQ allows accurate proteome-wide label-free quantification by delayed normalization and maximal peptide ratio extraction. Mol. Cell. Proteom. 13 (9), 2513–2526 mcp. M113. 031591.
Cui, Y., Yang, Y., Ni, Z., Dong, Y., Cai, G., Foncelle, A., et al., 2018. Astroglial Kir4.1 in the

lateral habenula drives neuronal bursts in depression. Nature. 554, 323–327.
Das, B., Conroy, M., Moore, D., Lysaght, J., McCrory, C., 2018. Human dorsal root ganglion pulsed radiofrequency treatment modulates cerebrospinal fluid lymphocytes and neuroinflammatory markers in chronic radicular pain. Brain Behav. Immun. 70, 157–165.
de Graaf, M.T., de Jongste, A.H., Kraan, J., Boonstra, J.G., Sillevis Smitt, P.A., Gratama, J.W., 2011a. Flow cytometric characterization of cerebrospinal fluid cells. Cytometry B Clin. Cytom. 80, 271–281.
de Graaf, M.T., Smitt, P.A., Luitwieler, R.L., van Velzen, C., van den Broek, P.D., Kraan, J., et al., 2011b. Central memory CD4+ T cells dominate the normal cerebrospinal fluid. Cytometry B Clin. Cytom. 80, 43–50.
De Ridder, D., Vanneste, S., 2016. Burst and tonic spinal cord stimulation: different and common brain mechanisms. Neuromodulation. 19, 47–59.
De Ridder, D., Vanneste, S., Plazier, M., van der Loo, E., Menovsky, T., 2010. Burst spinal cord stimulation: toward paresthesia-free pain suppression. Neurosurgery. 66, 986–990.
Deer, T.R., Levy, R.M., Kramer, J., Poree, L., Amirdelfan, K., Grigsby, E., et al., 2017. Dorsal root ganglion stimulation yielded higher treatment success rate for complex regional pain syndrome and causalgia at 3 and 12 months: a randomized comparative trial. Pain. 158, 669–681.
Deer, T., Slavin, K.V., Amirdelfan, K., North, R.B., Burton, A.W., Yearwood, T.L., et al., 2018. Success using neuromodulation with BURST (SUNBURST) study: results from a prospective, randomized controlled trial using a novel burst waveform. Neuromodulation. 21, 56–66.
Duffy, S.S., Keating, B.A., Perera, C.J., Moalem-Taylor, G., 2018. The role of regulatory T cells in nervous system pathologies. J. Neurosci. Res. 96, 951–968.
Fernyhough, P., Calcutt, N.A., 2010. Abnormal calcium homeostasis in peripheral neuropathies. Cell Calcium 47, 130–139.
Fields, R.D., Burnstock, G., 2006. Purinergic signalling in neuron-glia interactions. Nat. Rev. Neurosci. 7, 423–436.
Finnerup, N.B., Attal, N., Haroutounian, S., McNicol, E., Baron, R., Dworkin, R.H., et al., 2015. Pharmacotherapy for neuropathic pain in adults: a systematic review and meta-analysis. Lancet Neurol. 14, 162–173.
Grace, P.M., Hutchinson, M.R., Maier, S.F., Watkins, L.R., 2014. Pathological pain and the neuroimmune interface. Nat. Rev. Immunol. 14, 217–231.
Hagenston, A.M., Simonetti, M., 2014. Neuronal calcium signaling in chronic pain. Cell Tissue Res. 357, 407–426.
Hawker, G.A., Mian, S., Kendzerska, T., French, M., 2011. Measures of adult pain: Visual Analog Scale for Pain (VAS Pain), Numeric Rating Scale for Pain (NRS Pain), McGill Pain Questionnaire (MPQ), Short-Form McGill Pain Questionnaire (SF-MPQ), Chronic Pain Grade Scale (CPGS), Short Form-36 Bodily Pain Scale (SF-36 BPS), and Measure of Intermittent and Constant Osteoarthritis Pain (ICOAP). Arthritis Care Res. (Hoboken). 63 (Suppl. 11), S240–S252.
Hebb, A.L., Poulin, J.-F., Roach, S.P., Zacharko, R.M., Drolet, G., 2005. Cholecystokinin and endogenous opioid peptides: interactive influence on pain, cognition, and emotion. Prog. Neuro-Psychopharmacol. Biol. Psychiatry 29, 1225–1238.
Huang, J., Polgar, E., Solinski, H.J., Mishra, S.K., Tseng, P.Y., Iwagaki, N., et al., 2018. Circuit dissection of the role of somatostatin in itch and pain. Nat. Neurosci. 21, 707–716.
Hughes, C.S., Foehr, S., Garfield, D.A., Furlong, E.E., Steinmetz, L.M., Krijgsveld, J., 2014. Ultrasensitive proteome analysis using paramagnetic bead technology. Mol. Syst. Biol. 10, 757.
Hummert, M.W., Alvermann, S., Gingele, S., Gross, C.C., Wiendl, H., Mirenska, A., et al., 2018. Immunophenotyping of cerebrospinal fluid cells by Chipcytometry. J. Neuroinflammation 15, 160.
Hung, A.L., Lim, M., Doshi, T.L., 2017. Targeting cytokines for treatment of neuropathic pain. Scand J Pain 17, 287–293.
Inoue, K., Tsuda, M., 2018. Microglia in neuropathic pain: cellular and molecular mechanisms and therapeutic potential. Nat. Rev. Neurosci. 19, 138–152.
Jeon, S.Y., Seo, S., Lee, J.S., Choi, S.H., Lee, D.H., Jung, Y.H., et al., 2017. [11C]-(R)-PK11195 positron emission tomography in patients with complex regional pain syndrome: A pilot study. Medicine (Baltimore) 96, e5735.
Ji, R.R., Nackley, A., Huh, Y., Terrando, N., Maixner, W., 2018. Neuroinflammation and central sensitization in chronic and widespread pain. Anesthesiology. 129, 343–366.
Kapural, L., Yu, C., Doust, M.W., Gliner, B.E., Vallejo, R., Sitzman, B.T., et al., 2016. Comparison of 10-kHz high-frequency and traditional low-frequency spinal cord stimulation for the treatment of chronic Back and leg pain: 24-month results from a multicenter, randomized, controlled pivotal trial. Neurosurgery 79, 667–677.
Kettenmann, H., Kirchhoff, F., Verkhratsky, A., 2013. Microglia: new roles for the synaptic stripper. Neuron. 77, 10–18.
Khodorova, A., Montmayeur, J.P., Strichartz, G., 2009. Endothelin receptors and pain. J. Pain 10, 4–28.
Khoonsari, P.E., Musunri, S., Herman, S., Svensson, C.I., Tanum, L., Gordh, T., et al., 2019a. Systematic analysis of the cerebrospinal fluid proteome of fibromyalgia patients. J. Proteome 190, 35–43.
Khoonsari, P.E., Ossipova, E., Lengqvist, J., Svensson, C.I., Kosek, E., Kadetoff, D., et al., 2019b. The human CSF pain proteome. J. Proteome 190, 67–76.
Kinfe, T.M., Muhammad, S., Link, C., Roeske, S., Chaudhry, S.R., Yearwood, T.L., 2017. Burst spinal cord stimulation increases peripheral Antineuroinflammatory interleukin 10 levels in failed Back surgery syndrome patients with predominant Back pain. Neuromodulation. 20, 322–330.
Kinfe, T.M., Buchfelder, M., Chaudhry, S.R., Chakravarthy, K.V., Deer, T.R., Russo, M., et al., 2019. Leptin and associated mediators of Immunometabolic signaling: novel molecular outcome measures for Neurostimulation to treat chronic pain. Int. J. Mol. Sci. 20.
Kirketeig, T., Schultheis, C., Zuidema, X., Hunter, C.W., Deer, T., 2019. Burst spinal cord stimulation: a clinical review. Pain Med. 20, S31–S40.
Korvela, M., Lind, A.L., Wetterhall, M., Gordh, T., Andersson, M., Pettersson, J., 2016. Quantification of 10 elements in human cerebrospinal fluid from chronic pain patients with and without spinal cord stimulation. J. Trace Elem. Med. Biol. 37, 1–7.
Kothur, K., Wienholt, L., Brilot, F., Dale, R.C., 2016. CSF cytokines/chemokines as biomarkers in neuroinflammatory CNS disorders: a systematic review. Cytokine. 77, 227–237.
Krahe, R., Gabbiani, F., 2004. Burst firing in sensory systems. Nat. Rev. Neurosci. 5, 13–23.
Kriek, N., Schreurs, M.W.J., Groeneweg, J.G., Dik, W.A., Tjiang, G.C.H., Gultuna, I., et al., 2018. Spinal cord stimulation in patients with complex regional pain syndrome: a possible target for immunomodulation? Neuromodulation. 21, 77–86.
Krukowski, K., Eijkelkamp, N., Laumet, G., Hack, C.E., Li, Y., Dougherty, P.M., et al., 2016. CD8+ T cells and endogenous IL-10 are required for resolution of chemotherapy-induced neuropathic pain. J. Neurosci. 36, 11074–11083.
Lind, A.L., Emami Khoonsari, P., Sjodin, M., Katila, L., Wetterhall, M., Gordh, T., et al., 2016. Spinal cord stimulation alters protein levels in the cerebrospinal fluid of neuropathic pain patients: a proteomic mass spectrometric analysis. Neuromodulation. 19, 549–562.
Loggia, M.L., Chonde, D.B., Akeju, O., Arabasz, G., Catana, C., Edwards, R.R., et al., 2015. Evidence for brain glial activation in chronic pain patients. Brain. 138, 604–615.
Luchting, B., Rachinger-Adam, B., Heyn, J., Hinske, L.C., Kreth, S., Azad, S.C., 2015. Anti-inflammatory T-cell shift in neuropathic pain. J. Neuroinflammation 12, 12.
Maxeiner, H.G., Rojewski, M.T., Schmitt, A., Tumani, H., Bechter, K., Schmitt, M., 2009. Flow cytometric analysis of T cell subsets in paired samples of cerebrospinal fluid and peripheral blood from patients with neurological and psychiatric disorders. Brain Behav. Immun. 23, 134–142.
McCarthy, K.F., McCrory, C., 2014. Cerebrospinal fluid levels of glial cell-derived neurotrophic factor correlate with spinal cord stimulation frequency in patients with neuropathic pain: a preliminary report. Spinal Cord 52 (Suppl. 2), S8–10.
McCarthy, K.F., Connor, T.J., McCrory, C., 2013. Cerebrospinal fluid levels of vascular endothelial growth factor correlate with reported pain and are reduced by spinal cord stimulation in patients with failed back surgery syndrome. Neuromodulation. 16, 519–522 (discussion 22).
Meacham, K., Shepherd, A., Mohapatra, D.P., Haroutounian, S., 2017. Neuropathic pain: central vs. peripheral mechanisms. Curr. Pain Headache Rep. 21, 28.
Mei, Y., Barrett, J.E., Hu, H., 2018. Calcium release-activated calcium channels and pain. Cell Calcium 74, 180–185.
Mekhail, N., Levy, R.M., Deer, T.R., Kapural, L., Li, S., Amirdelfan, K., et al., 2019. Long-term safety and efficacy of closed-loop spinal cord stimulation to treat chronic back and leg pain (Evoke): a double-blind, randomised, controlled trial. Lancet Neurol. 19 (2), 123–134.
Muhammad, S., Chaudhry, S.R., Yearwood, T.L., Krauss, J.K., Kinfe, T.M., 2018. Changes of metabolic disorders associated peripheral cytokine/Adipokine traffic in non-obese chronic Back patients responsive to burst spinal cord stimulation. Neuromodulation. 21, 31–37.
Murphy, D.M., O'Callaghan, D.S., Gaine, S.P., 2010. Relief of chronic neuropathic pain through endothelin antagonism. Am. J. Med. 123, e7.
Mzhavia, N., Berman, Y., Che, F.-Y., Fricker, L.D., Devi, L.A., 2001. ProSAAS processing in mouse brain and pituitary. J. Biol. Chem. 276, 6207–6213.
Mzhavia, N., Qian, Y., Feng, Y., Che, F.Y., Devi, L.A., Fricker, L.D., 2002. Processing of proSAAS in neuroendocrine cell lines. Biochem. J. 361, 67–76.
Navarrete, M., Perea, G., Maglio, L., Pastor, J., Garcia de Sola, R., Araque, A., 2013. Astrocyte calcium signal and gliotransmission in human brain tissue. Cereb. Cortex 23, 1240–1246.
Perea, G., Araque, A., 2005. Glial calcium signaling and neuron-glia communication. Cell Calcium 38, 375–382.
Remy, S., Spruston, N., 2007. Dendritic spikes induce single-burst long-term potentiation. Proc. Natl. Acad. Sci. U. S. A. 104, 17192–17197.
Ren, K., Ruda, M.A., 1994. A comparative study of the calcium-binding proteins calbindin-D28K, calretinin, calmodulin and parvalbumin in the rat spinal cord. Brain Res. Brain Res. Rev. 19, 163–179.
Rowlingson, J.C., 2007. Cholecystokinin and its antagonists in pain management. Anesth. Analg. 104, 750.
Ruiz-Sauri, A., Orduna-Valls, J.M., Blasco-Serra, A., Tornero-Tornero, C., Cedeno, D.L., Bejarano-Quisoboni, D., et al., 2019. Glia to neuron ratio in the posterior aspect of the human spinal cord at thoracic segments relevant to spinal cord stimulation. J. Anat. 235 (5), 997–1006.
Rupprecht, R., Papadopoulos, V., Rammes, G., Baghai, T.C., Fan, J., Akula, N., et al., 2010. Translocator protein (18 kDa) (TSPO) as a therapeutic target for neurological and psychiatric disorders. Nat. Rev. Drug Discov. 9, 971–988.
Salter, M.W., Beggs, S., 2014. Sublime microglia: expanding roles for the guardians of the CNS. Cell. 158, 15–24.
Schutzer, S.E., Liu, T., Natelson, B.H., Angel, T.E., Schepmoes, A.A., Purvine, S.O., et al., 2010. Establishing the proteome of normal human cerebrospinal fluid. PLoS One 5, e10980.
Schwaller, B., Meyer, M., Schiffmann, S., 2002. 'New' functions for 'old' proteins: the role of the calcium-binding proteins calbindin D-28k, calretinin and parvalbumin, in cerebellar physiology. Studies with knockout mice. Cerebellum. 1, 241–258.
Seybold, V., Hylden, J., Wilcox, G., 1982. Intrathecal substance P and somatostatin in rats: behaviors indicative of sensation. Peptides. 3, 49–54.
Sherman, S.M., 2001. Tonic and burst firing: dual modes of thalamocortical relay. Trends Neurosci. 24, 122–126.
Shi, T.J., Xiang, Q., Zhang, M.D., Barde, S., Kai-Larsen, Y., Fried, K., et al., 2014. Somatostatin and its 2A receptor in dorsal root ganglia and dorsal horn of mouse and human: expression, trafficking and possible role in pain. Mol. Pain 10, 12.

Smith, T.P., Haymond, T., Smith, S.N., Sweitzer, S.M., 2014. Evidence for the endothelin system as an emerging therapeutic target for the treatment of chronic pain. J. Pain Res. 7, 531–545.
Sorge, R.E., Mapplebeck, J.C., Rosen, S., Beggs, S., Taves, S., Alexander, J.K., et al., 2015. Different immune cells mediate mechanical pain hypersensitivity in male and female mice. Nat. Neurosci. 18, 1081–1083.
Stephens, K.E., Chen, Z., Sivanesan, E., Raja, S.N., Linderoth, B., Taverna, S.D., et al., 2018. RNA-seq of spinal cord from nerve-injured rats after spinal cord stimulation. Mol. Pain 14 1744806918817429.
Subira, D., Castanon, S., Aceituno, E., Hernandez, J., Jimenez-Garofano, C., Jimenez, A., et al., 2002. Flow cytometric analysis of cerebrospinal fluid samples and its usefulness in routine clinical practice. Am. J. Clin. Pathol. 117, 952–958.
Swadlow, H.A., Gusev, A.G., 2001. The impact of 'bursting' thalamic impulses at a neocortical synapse. Nat. Neurosci. 4, 402–408.
Tagaya, Y., Miura, A., Okada, S., Ohshima, K., Mori, M., 2012. Nucleobindin-2 is a positive modulator of EGF-dependent signals leading to enhancement of cell growth and suppression of adipocyte differentiation. Endocrinology. 153, 3308–3319.
Tang, W., Lv, Q., Chen, X.F., Zou, J.J., Liu, Z.M., Shi, Y.Q., 2013. CD8(+) T cell-mediated cytotoxicity toward Schwann cells promotes diabetic peripheral neuropathy. Cell. Physiol. Biochem. 32, 827–837.
ten Bokum, A.M., Hofland, L., van Hagen, P.M., 2000. Somatostatin and somatostatin receptors in the immune system: a review. Eur. Cytokine Netw. 11, 161–176.
Tjepkema-Cloostermans, M.C., de Vos, C.C., Wolters, R., Dijkstra-Scholten, C., Lenders, M.W., 2016. Effect of burst stimulation evaluated in patients familiar with spinal cord stimulation. Neuromodulation. 19, 492–497.
Totsch, S.K., Sorge, R.E., 2017. Immune system involvement in specific pain conditions. Mol. Pain 13 1744806917724559.
Tsuda, M., Koga, K., Chen, T., Zhuo, M., 2017. Neuronal and microglial mechanisms for neuropathic pain in the spinal dorsal horn and anterior cingulate cortex. J. Neurochem. 141, 486–498.
Ullian, E.M., Christopherson, K.S., Barres, B.A., 2004. Role for glia in synaptogenesis. Glia. 47, 209–216.
Vachon-Presseau, E., 2018. Effects of stress on the corticolimbic system: implications for chronic pain. Prog. Neuro-Psychopharmacol. Biol. Psychiatry 87, 216–223.
Vallejo, R., Bradley, K., Kapural, L., 2017. Spinal cord stimulation in chronic pain: mode of action. Spine (Phila Pa 1976) 42 (Suppl. 14), S53–S60.
van Hecke, O., Kamerman, P.R., Attal, N., Baron, R., Bjornsdottir, G., Bennett, D.L., et al., 2015. Neuropathic pain phenotyping by international consensus (NeuroPPIC) for genetic studies: a NeuPSIG systematic review, Delphi survey, and expert panel recommendations. Pain. 156, 2337–2353.
Vesper, J., Slotty, P., Schu, S., Poeggel-Kraemer, K., Littges, H., Van Looy, P., et al., 2019. Burst SCS microdosing is as efficacious as standard burst SCS in treating chronic Back and leg pain: results from a randomized controlled trial. Neuromodulation. 22, 190–193.
Weinand, M.E., Madhusudan, H., Davis, B., Melgar, M., 2003. Acute vs. prolonged screening for spinal cord stimulation in chronic pain. Neuromodulation. 6, 15–19.
Wiesenfeld-Hallin, Z., 1985. Intrathecal somatostatin modulates spinal sensory and reflex mechanisms: behavioral and electrophysiological studies in the rat. Neurosci. Lett. 62, 69–74.
Xu, J., Casserly, E., Yin, Y., Cheng, J., 2019. A systematic review of growth hormone in pain medicine: from rodents to humans. Pain Med. 21 (1), 21–31.
Yang, M., Shi, X.Q., Peyret, C., Oladiran, O., Wu, S., Chambon, J., et al., 2018. Effector/memory CD8(+) T cells synergize with co-stimulation competent macrophages to trigger autoimmune peripheral neuropathy. Brain Behav. Immun. 71, 142–157.
Yearwood, T., De Ridder, D., Yoo, H.B., Falowski, S., Venkatesan, L., Ting To, W., et al., 2019. Comparison of neural activity in chronic pain patients during tonic and burst spinal cord stimulation using fluorodeoxyglucose positron emission tomography. Neuromodulation 23 (1), 56–63.
Zhang, J.-M., An, J., 2007. Cytokines, inflammation and pain. Int. Anesthesiol. Clin. 45, 27.
Zhao, H., Alam, A., Chen, Q., Eusman, M.A., Pal, A., Eguchi, S., et al., 2017. The role of microglia in the pathobiology of neuropathic pain development: what do we know? Br. J. Anaesth. 118, 504–516.